


Haralick's texture features for the prediction of response to therapy in colorectal cancer: a preliminary study

Damiano Caruso¹ · Marta Zerunian¹ · Maria Ciolina¹ · Domenico de Santis¹ · Marco Rengo¹ · Mumtaz H. Soomro² · Gaetano Giunta² · Silvia Conforto² · Maurizio Schmid² · Emanuele Neri³ · Andrea Laghi¹ 

Received: 31 August 2017 / Accepted: 2 November 2017 / Published online: 8 November 2017
© Italian Society of Medical Radiology 2017

Abstract

Purpose Haralick features Texture analysis is a recent oncologic imaging biomarker used to assess quantitatively the heterogeneity within a tumor. The aim of this study is to evaluate which Haralick's features are the most feasible in predicting tumor response to neoadjuvant chemoradiotherapy (CRT) in colorectal cancer.

Materials and Methods After MRI and histological assessment, eight patients were enrolled and divided into two groups based on response to neoadjuvant CRT in complete responders (CR) and non-responders (NR). Oblique Axial T2-weighted MRI sequences before CRT were analyzed by two radiologists in consensus drawing a ROI around the tumor. 14 over 192 Haralick's features were extrapolated from normalized gray-level co-occurrence matrix in four different directions. A dedicated statistical analysis was performed to evaluate distribution of the extracted Haralick's features computing mean and standard deviation.

Results Pretreatment MRI examination showed significant value ($p < 0.05$) of 5 over 14 computed Haralick texture. In particular, the significant features are the following: concerning energy, contrast, correlation, entropy and inverse difference moment.

Conclusions Five Haralick's features showed significant relevance in the prediction of response to therapy in colorectal cancer and might be used as additional imaging biomarker in the oncologic management of colorectal patients.

Keywords T2-weighted MRI · Colorectal cancer · Haralick's texture analysis · Response to therapy

Introduction

Early diagnosis and accurate staging of rectal cancer are raising an essential role in the oncologic patients' management particularly in personalized treatment strategies. Nowadays, magnetic resonance imaging (MRI) is considered the imaging modality of choice for loco-regional staging of rectal cancer [1, 2]. The validation of the technique for this purpose has been based on the ability to distinguish normal rectal wall from pathologic tissues on the basis of the high contrast resolution achievable on T2-weighted sequences [3]. However, its role in the evaluation of response to therapy is challenging due to the difficulty in discriminating fibrotic to viable residual tissue after neoadjuvant chemoradiotherapy (CRT) through morphologic approach with T2-weighted image [4].

Visual assessment has several limitations compared to quantitative measurements, such as inferior inter-reader agreement due to human eye error [5]. To overcome this issue, a multiparametric approach [6, 7] including T2-weighted, diffusion-weighted images (DWI) [8–10] and dynamic contrast-enhanced MRI (DCE-MRI) have been proposed [11, 12] with improved results but not already optimal to assure a personalized treatment to patients. Moreover, multiparametric MRI morphological assessment cannot assess the tumor at the cellular level.

✉ Andrea Laghi
andrea.laghi@uniroma1.it

¹ Department of Radiological Sciences, Oncology and Pathology, "Sapienza" - University of Rome, I.C.O.T. Hospital, Via Franco Faggiana 1668, 04100 Latina, Italy

² Department of Engineering, University of Roma Tre, Via Vito Volterra 62, 00146 Rome, Italy

³ Department of Radiological Sciences, AOUP, Via Savi 10, 56126 Pisa, Italy

Taking into account the weaknesses in visual process, there is the need to find new accurate quantitative semi-automatic/automatic diagnostics techniques [13]. Recently, new MRI biomarkers, such as Texture analysis, were investigated. Texture analysis is a non-invasive method to evaluate tissue heterogeneity of tumor lesions [14]. In literature, Texture parameters derived from T2-weighted images of rectal cancer have the potential role as imaging biomarkers of tumoral response to neoadjuvant CRT [15]. Texture analysis evaluates the spatial variation of gray levels within an image, through mathematical equations that generate several parameters associated with the Texture of an image. It is possible to extract Texture parameters using statistical (first-order, second-order, and high-order), model-based or transform methods [16]. In particular, Haralick's Texture analysis, known as the spatial gray-level dependence matrix method, let the study of second-order statistics of pixels at different spacings and angles of adjacent or nearest-neighbor pixels [17, 18]; this statistical method reflects the spatial and signal intensity interrelationships between adjacent in-plane voxels (e.g. contrast, homogeneity, second-order entropy and energy), useful for a quantitative analysis of the tissue corresponding to different histology observed for instance in fibrotic tissue instead of viable residual tumor [19].

An early prediction of patients who can respond to therapy or not should be advisable in future target and it will allow a considerable change in patients' treatment management. Thus, the purpose of this paper was to determine which of the quantitative parameters extrapolated from

Haralick's Texture analysis most suitable in predicting complete tumor response to neoadjuvant therapy and to evaluate the possible correlation among these parameters.

Materials and methods

Population study

This retrospective study involved a sub-cohort of prospectively enrolled patients involved in the Italian Association for Cancer Research (AIRC) trial study "MR Imaging Biomarkers in Response Evaluation to Neoadjuvant Chemoradiotherapy in Rectal Cancer" I.G. 2013/14129. The investigation was approved by our institutional ethics committee and all patients gave written informed consent. All patients had histologically proved colorectal adenocarcinoma and locally advanced tumor stage from II (cT3-4, N0, M0) to III (cT2-4, N + , M0) following the UICC 2009. Exclusion criteria were considered the following: (a) patients with a histological partial response to therapy; (b) patients who have not completed the neoadjuvant treatment (e.g. hypersensitivity to the study drugs); (c) patients who have not been surgically treated, thus histological results are not available; (d) patients treated with concurrent and experimental drugs or participation in another clinical trial. Patients selected were divided into two groups based on response to treatment as complete responder (CR) and non-responder (NR), as shown in Fig. 1.

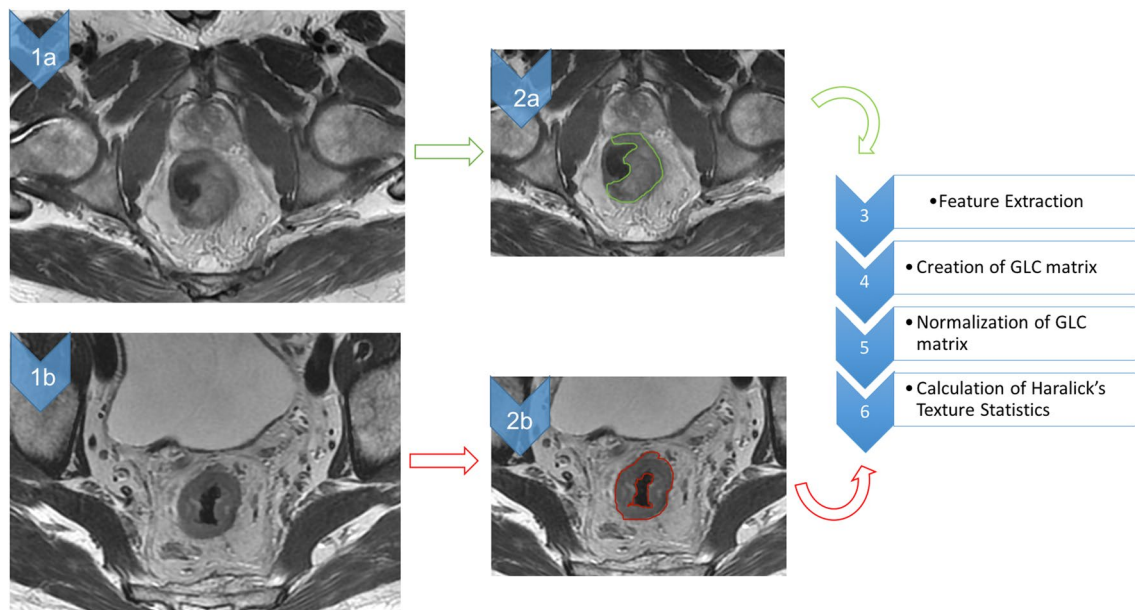


Fig. 1 Flow chart of methodology: data were organized into two categories by visual inspection of radiologists (**1a** and **1b**); manual segmentation of complete responder (**2a**, green line) and Non-Responder

(**2b**, red line) was performed; after manual segmentation, each MRI was elaborated to extrapolate Haralick's Texture data (from 3 to 6)

Study protocol

All patients underwent 3 MRI examinations, as have been already extensively described in another study [14]. MRI scanning were executed before, during and after neoadjuvant therapy. Between 6 and 8 weeks after the CRT, total mesorectal excision (TME) was performed and an experienced pathologist analyzed the gross specimen. Due to the specific purpose of this study, we have focused our analyses only on pretreatment Oblique Axial T2-weighted MRI examinations for the assessment of imaging biomarkers capable to discriminate from responder and non-responder patients prior to the beginning of neoadjuvant therapy.

MRI examination

All MRI acquisitions were performed using a 3T scanner (Discovery MR750, General Electrics, Milwaukee, Wisconsin, USA). A standard clinical imaging protocol used for rectal cancer study was performed including routinely and dedicated sequences, such as T1 and T2-weighted with fat saturation/suppression, DWI, ADC and dynamic contrast-enhanced sequences as described in another study [15]. For the specific purpose of our study, we analyzed high-resolution T2-weighted fast recovery fast-spin echo (2D FRFSE) sequence (TR, 2086–4172 ms; TE, 11.4–122.3 ms; Nex, 2; slice thickness, 4 mm; matrix, 512 × 512) acquired angled to the axial planes orthogonal to the long axis of the rectum to obtain an Oblique Axial T2-weighted planes [19–21]. High-resolution T2-weighted images grant an optimal morphologic evaluation by allowing a precise tumor segmentation; additionally, the texture parameters have a good reproducibility on T2-weighted as described in literature [19, 22].

Texture analysis

Haralick's texture analysis is a statistical technique, known as the spatial gray-level dependence matrix method. Using it is possible to study second-order statistics of pixels at different spacings and direction of adjacent or nearest-neighbor pixels. As Freeborough and Fox demonstrated [23], a Texture discriminant function derived from MRI brain scans using a spoiled gradient-echo technique on a 1.5 T system gave significantly different values for Alzheimer sufferers compared to normal controls [17].

Two radiologists (XXX and XXX) with 7 and 11 years of experience in rectal cancer MRI evaluation, respectively, performed the segmentation step in consensus. The tumor region has been manually drawn from pre-CRT oblique Axial T2-weighted MRI image, slice by slice for the entire tumor volume by means of a free open-source segmentation platform (ITK-SNAP version 4.11.0; www.itk-snap.org) [24, 25]. After the segmentation process,

segmented images were computed with Haralick's textural analysis method [18] as described by Soomro et al. 2017 [26] for feature extraction (Fig. 1).

Based on previous study, 14 Haralick's Texture features were selected over 192 total features as shown in Table 1, and every segmented ROI have been computed from normalized gray-level co-occurrence matrix (GLC) in the four main direction (viz: 0°, 45°, 90° and 135°) [18].

The entire volume of the tumor was computed at each voxel with Gray level co-occurrence matrices (GLCM) and the selected features were extracted. GLCM can be mainly described as an histogram in two dimension that assesses the co-occurrence frequency of two pixel intensities at a specified offset compared to each other over the region where the texture is computed. Each texture feature computes a specific relation of pixels with their local neighborhood [27]. In detail, *Energy* provides knowledge about uniformity of image with a 0–1 range (the highest value 1 expresses low variation in image with respect to intensity). *Contrast* measures local fluctuation: its high value indicates the higher intensity variation among pixels in the image. *Correlation* recognizes the parallelism among image gray levels with values between – 1 and + 1 where + 1 indicates a higher linear dependencies of image gray levels. The chaotic distribution of image gray levels was quantified by *Entropy*. At last, *inverse difference moment* is referred to as uniformity quantifying the affinity of co-occurrence gray levels [26].

Table 1 14 Haralick's texture features analyzed are described in Table 1

Haralick's texture features	
1	Energy
2	Contrast
3	Sum of squares
4	Correlation
5	Sum average
6	Inverse difference Moment or homogeneity
7	Entropy
8	Sum variance
9	Sum entropy
10	Difference variance
11	Difference entropy
12	Information measure correlation—1
13	Information measure correlation—2
14	Maximum correlation

In bold are reported the 5 over 14 features that shown significant results

Statistical analysis

To evaluate distribution of the extracted Haralick's features, statistical analysis was performed computing mean and standard deviation using Statistical analysis with SPSS (21.0; SPSS, Chicago, IL, USA) and MedCalc version 12.7.2 (MedCalc Software, Ostend, Belgium). Dedicated engineers performed a normalization of the GLC matrices by taking the neighbor pixel values and reference pixel values paying attention to probability rather than just counting of co-occurrences as suggested Wibmer and colleagues [27]. Data obtained were matched with clinical data as well as histological evaluation. Linear regression was performed to evaluate the association between texture parameters and histological results. The Wald test from the regression model was performed and p values ≤ 0.05 were considered statistically significant.

Results

From a total of 90 consecutive patients enrolled in the aforementioned trial, 82 patients were excluded due to: (a) histological partial response to therapy ($n = 21$); (b) non-completion of the neoadjuvant treatment at the time of the present study ($n = 46$); (c) lack of surgical treatment ($n = 2$); and (d) lack of histological results at the time of patient selection ($n = 13$).

Thus, the final population consisted of eight patients (two females, six males, median age 65.5 years, range 58–78 years) with locally advanced colorectal adenocarcinoma at tumor stages II (cT3-4, N0, M0) and III (cT2-4, N + , M0) confirmed by preliminary biopsy. All patients follow a neoadjuvant CRT and after a time-span of 6-8 weeks, they underwent Total Mesorectal Excision surgery (TME) followed by the histological assessment performed by an expert gastrointestinal pathologist.

Preliminary results on Haralick's Texture analysis has shown that 5 over 14 features could hire an important role as MRI biomarker to differentiate between complete responder and non-responder patients affected by rectal cancer (all $p < 0.05$): *Energy*, *Contrast*, *Correlation*, *Entropy*, *inverse difference moment*. CR patients have significantly higher values of *energy*, *correlation* and *inverse difference moment* features in comparison with NR (all $p < 0.05$), whereas *contrast* and *entropy* show significantly lower values for CR compared to NR (all $p < 0.05$). Moreover, no significant differences among all the directions were observed within the same group (all $p > 0.05$). Full data are reported in Table 2 and Fig. 2.

Table 2 Data are reported as mean \pm standard deviation

Haralick's texture features	Complete responder						Non-responder						P values										
	0°		45°		90°		135°		45°		90°		135°		0°		45°		90°		135°		
	Mean	SD	Mean	SD	Mean	SD	Mean	SD	Mean	SD	Mean	SD	Mean	SD	Mean	SD	Mean	SD	Mean	SD	Mean	SD	
Energy	0.875 \pm 0.043	0.915 \pm 0.029	0.882 \pm 0.073	0.918 \pm 0.028	0.882 \pm 0.029	0.882 \pm 0.029	0.882 \pm 0.029	0.882 \pm 0.029	0.882 \pm 0.029	0.882 \pm 0.029	0.882 \pm 0.029	0.882 \pm 0.029	0.882 \pm 0.029	0.882 \pm 0.029	0.882 \pm 0.029	0.882 \pm 0.029	0.882 \pm 0.029	0.882 \pm 0.029	0.882 \pm 0.029	0.882 \pm 0.029	0.882 \pm 0.029	0.882 \pm 0.029	0.882 \pm 0.029
Contrast	0.066 \pm 0.014	0.070 \pm 0.041	0.066 \pm 0.021	0.054 \pm 0.029	0.066 \pm 0.021	0.066 \pm 0.021	0.066 \pm 0.021	0.066 \pm 0.021	0.066 \pm 0.021	0.066 \pm 0.021	0.066 \pm 0.021	0.066 \pm 0.021	0.066 \pm 0.021	0.066 \pm 0.021	0.066 \pm 0.021	0.066 \pm 0.021	0.066 \pm 0.021	0.066 \pm 0.021	0.066 \pm 0.021	0.066 \pm 0.021	0.066 \pm 0.021	0.066 \pm 0.021	0.066 \pm 0.021
Correlation	0.890 \pm 0.082	0.795 \pm 0.097	0.922 \pm 0.061	0.870 \pm 0.063	0.922 \pm 0.061	0.922 \pm 0.061	0.922 \pm 0.061	0.922 \pm 0.061	0.922 \pm 0.061	0.922 \pm 0.061	0.922 \pm 0.061	0.922 \pm 0.061	0.922 \pm 0.061	0.922 \pm 0.061	0.922 \pm 0.061	0.922 \pm 0.061	0.922 \pm 0.061	0.922 \pm 0.061	0.922 \pm 0.061	0.922 \pm 0.061	0.922 \pm 0.061	0.922 \pm 0.061	0.922 \pm 0.061
Entropy	0.229 \pm 0.072	0.202 \pm 0.146	0.222 \pm 0.024	0.267 \pm 0.068	0.222 \pm 0.024	0.222 \pm 0.024	0.222 \pm 0.024	0.222 \pm 0.024	0.222 \pm 0.024	0.222 \pm 0.024	0.222 \pm 0.024	0.222 \pm 0.024	0.222 \pm 0.024	0.222 \pm 0.024	0.222 \pm 0.024	0.222 \pm 0.024	0.222 \pm 0.024	0.222 \pm 0.024	0.222 \pm 0.024	0.222 \pm 0.024	0.222 \pm 0.024	0.222 \pm 0.024	0.222 \pm 0.024
IDM	0.767 \pm 0.042	0.792 \pm 0.023	0.770 \pm 0.027	0.822 \pm 0.068	0.770 \pm 0.027	0.770 \pm 0.027	0.770 \pm 0.027	0.770 \pm 0.027	0.770 \pm 0.027	0.770 \pm 0.027	0.770 \pm 0.027	0.770 \pm 0.027	0.770 \pm 0.027	0.770 \pm 0.027	0.770 \pm 0.027	0.770 \pm 0.027	0.770 \pm 0.027	0.770 \pm 0.027	0.770 \pm 0.027	0.770 \pm 0.027	0.770 \pm 0.027	0.770 \pm 0.027	0.770 \pm 0.027

Complete responder showed superior results for *energy*, *correlation* and *inverse difference moment* features compared to non responder, whereas *contrast* and *entropy* showed significantly lower values for CR compared to NR. No significant differences were observed among all the directions examined within the same group

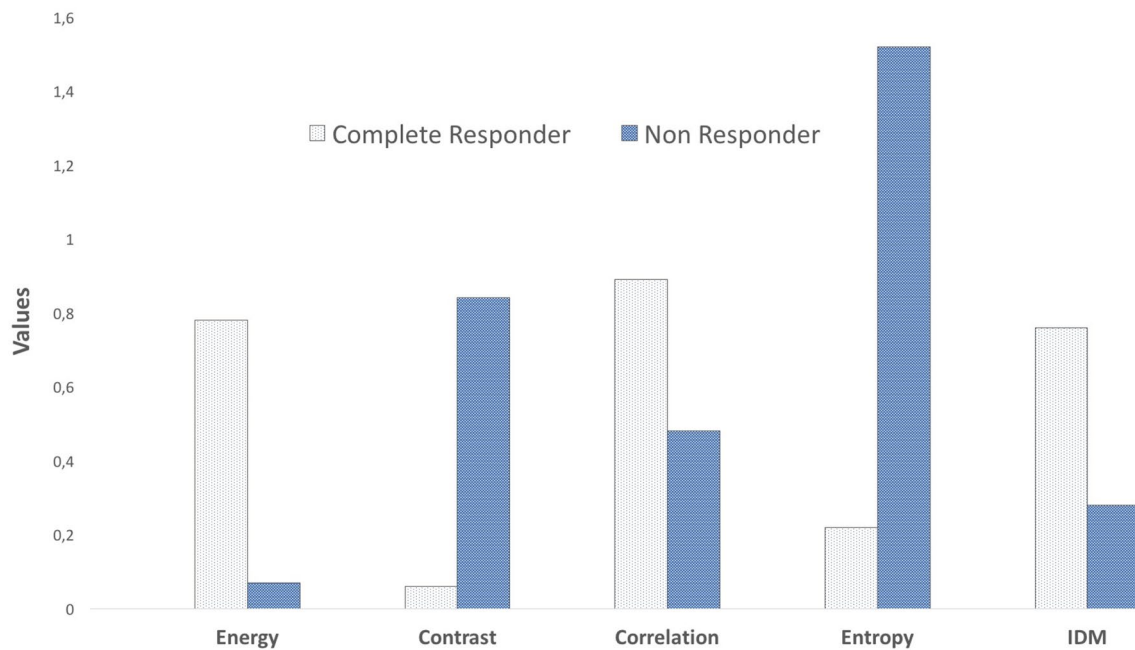


Fig. 2 Comparison between complete responder and non-responder Haralick's features

Discussion

This paper represents a preliminary technical study on Haralick's textural features and the possibly to evaluate the prognostic trend of colorectal cancer with MRI semi-automatic image analysis.

The T2-weighted colorectal MRI of CR patients showed less disorder and randomness than NR patients imaging. Moreover, T2-weighted images of CR patients have higher energy, inverse difference moment and correlation values, indicating uniformity in image, as well as lower entropy and contrast values, revealing lower randomness and dissimilarity in their gray levels in comparison with NR patients. Contrariwise, T2-weighted images of NR patients have higher entropy and contrast, representing higher randomness or disorder and dissimilarity in image gray levels.

Texture Analysis can be included in a wider field of research called Radiomics that has the aim to exploit the full potential of medical imaging [28]. As some studies described, radiomic signature identifies a general prognostic tumor phenotype, for instance in lung and head and neck tumor [29]. Moreover, with the integration of genomics and microarray could built the basis of a wider diagnostic branch called radiogenomic [30], a potential powerful tool for clinical decision able to assess, with higher accuracy than each single diagnostic tool, the response to neoadjuvant therapy or the tailored treatment based on the tumor phenotype leading to an overall improvement of patient management.

As demonstrated by Ng et al. [31], texture analysis allows the evaluation of the heterogeneity within a tumor. Recent

studies demonstrated that texture parameters derived from T2-weighted images of rectal cancer potentially might assume a role as imaging biomarkers in detecting tumoral response to neoadjuvant CRT [14]. Their capability on reflecting tumor heterogeneity may be further used in clinical practice, integrated to the other diagnostic tools, to improve the selection of tailored patients' therapy to avoid under/over treatment that could slow down the care process. Haralick analysis has been preferred in our study for the reasons as follow: first, fractal-based Texture models are computationally intensive as the model is estimated during the Texture extraction process; second, there is a lack in orientation sensitivity and these models are not suitable for describing local image structures [27].

Our study has several limitations. First, due to the technical purpose our results have been achieved in a small population retrospectively analyzed and should be confirmed with a more representative population. Second, we did not analyze with Haralick's Texture other MRI sequences as DWI, ADC or MRI perfusion. Third, we did not perform a proper 3D volumetric Texture evaluation because the software available allows only a single-slice evaluation contrarily to the Texture Analysis described by Wibmer et al. [27]. More studies are encouraged for a deeper analysis of the topic.

Conclusion

Our preliminary results showed that *energy*, *contrast*, *correlation*, *entropy* and *inverse difference moment*, are the

Haralick's features that may have a significant relevance in predicting the response to therapy in patients with colorectal cancer. In particular, the association of such imaging features with additional genomics and microarray data can potentially provide a comprehensive overview of tumor characteristics, allowing for an effective targeted therapy and moving towards a personalized treatment in patients with rectal cancer. Further prospective multicentre trials are advisable to achieve a large-scale validation of our results in clinical practice.

Acknowledgments This study is funded by AIRC (Associazione Italiana per la Ricerca sul Cancro) Investigator Grant 2013/14129.

Compliance with ethical standards

Conflict of interest The Authors declare that they have no conflict of interest.

Ethical standards All human and animal studies have been approved by the appropriate ethics committee and have therefore been performed in accordance with the ethical standards laid down in the 1964 Declaration of Helsinki and its later amendments or comparable ethical standards.

Informed consent All patients gave their informed consent prior to their inclusion in the study.

References

1. Beets-Tan RG, Lambregts DM, Maas M, Bipat S, Barbaro B, Caseiro-Alves F, Curvo-Semedo L, Fenlon HM, Gollub MJ, Gourtsoyianni S, Halligan S, Hoeffel C, Kim SH, Laghi A, Maier A, Rafaelsen SR, Stoker J, Taylor SA, Torkzad MR, Blomqvist L (2013) Magnetic resonance imaging for the clinical management of rectal cancer patients: recommendations from the 2012 European Society of Gastrointestinal and Abdominal Radiology (ESGAR) consensus meeting. *Eur Radiol* 23(9):2522–2531. <https://doi.org/10.1007/s00330-013-2864-4>
2. Laghi A, Ferri M, Catalano C, Baeli I, Iannaccone R, Iafrate F, Ziparo V, Passariello R (2002) Local staging of rectal cancer with MRI using a phased array body coil. *Abdom Imaging* 27(4):425–431. <https://doi.org/10.1107/s00261-001-0123-7>
3. Group MS (2006) Diagnostic accuracy of preoperative magnetic resonance imaging in predicting curative resection of rectal cancer: prospective observational study. *BMJ* 333(7572):779. <https://doi.org/10.1136/bmj.38937.646400.55>
4. van den Broek JJ, van der Wolf FS, Lahaye MJ, Heijnen LA, Meischl C, Heitbrink MA, Schreurs WH (2017) Accuracy of MRI in restaging locally advanced rectal cancer after preoperative chemoradiation. *Dis Colon Rectum* 60(3):274–283. <https://doi.org/10.1097/dcr.0000000000000743>
5. Maas M, Lambregts DM, Lahaye MJ, Beets GL, Backes W, Vliegen RF, Osinga-de Jong M, Wildberger JE, Beets-Tan RG (2012) T-staging of rectal cancer: accuracy of 3.0 Tesla MRI compared with 1.5 Tesla. *Abdom Imaging* 37(3):475–481. <https://doi.org/10.1007/s00261-011-9770-5>
6. Attenberger UI, Pilz LR, Morelli JN, Hausmann D, Doyon F, Hofheinz R, Kienle P, Post S, Michaely HJ, Schoenberg SO, Dinter DJ (2014) Multi-parametric MRI of rectal cancer—do quantitative functional MR measurements correlate with radiologic and pathologic tumor stages? *Eur J Radiol* 83(7):1036–1043. <https://doi.org/10.1016/j.ejrad.2014.03.012>
7. Hotker AM, Tarlinton L, Mazaheri Y, Woo KM, Gonen M, Saltz LB, Goodman KA, Garcia-Aguilar J, Gollub MJ (2016) Multiparametric MRI in the assessment of response of rectal cancer to neoadjuvant chemoradiotherapy: a comparison of morphological, volumetric and functional MRI parameters. *Eur Radiol* 26(12):4303–4312. <https://doi.org/10.1007/s00330-016-4283-9>
8. Curvo-Semedo L, Lambregts DM, Maas M, Beets GL, Caseiro-Alves F, Beets-Tan RG (2012) Diffusion-weighted MRI in rectal cancer: apparent diffusion coefficient as a potential noninvasive marker of tumor aggressiveness. *J Magn Reson Imaging JMIR* 35(6):1365–1371. <https://doi.org/10.1002/jmri.23589>
9. Jung SH, Heo SH, Kim JW, Jeong YY, Shin SS, Soung MG, Kim HR, Kang HK (2012) Predicting response to neoadjuvant chemoradiation therapy in locally advanced rectal cancer: diffusion-weighted 3 Tesla MR imaging. *J Magn Reson Imaging JMIR* 35(1):110–116. <https://doi.org/10.1002/jmri.22749>
10. Cai PQ, Wu YP, An X, Qiu X, Kong LH, Liu GC, Xie CM, Pan ZZ, Wu PH, Ding PR (2014) Simple measurements on diffusion-weighted MR imaging for assessment of complete response to neoadjuvant chemoradiotherapy in locally advanced rectal cancer. *Eur Radiol* 24(11):2962–2970. <https://doi.org/10.1007/s00330-014-3251-5>
11. Intven M, Reerink O, Philippens ME (2015) Dynamic contrast enhanced MR imaging for rectal cancer response assessment after neo-adjuvant chemoradiation. *J Magn Reson Imaging JMIR* 41(6):1646–1653. <https://doi.org/10.1002/jmri.24718>
12. Gollub MJ, Gultekin DH, Akin O, Do RK, Fuqua JL 3rd, Gonen M, Kuk D, Weiser M, Saltz L, Schrag D, Goodman K, Paty P, Guillem J, Nash GM, Temple L, Shia J, Schwartz LH (2012) Dynamic contrast enhanced-MRI for the detection of pathological complete response to neoadjuvant chemotherapy for locally advanced rectal cancer. *Eur Radiol* 22(4):821–831. <https://doi.org/10.1007/s00330-011-2321-1>
13. Hamilton PW, Bartels PH, Thompson D, Anderson NH, Montironi R, Sloan JM (1997) Automated location of dysplastic fields in colorectal histology using image texture analysis. *J Pathol* 182(1):68–75. [https://doi.org/10.1002/\(sici\)1096-9896\(199705\)182:1<68:aid-path811>3.0.co;2-n](https://doi.org/10.1002/(sici)1096-9896(199705)182:1<68:aid-path811>3.0.co;2-n)
14. De Cecco CN, Ganeshan B, Ciolina M, Rengo M, Meinel FG, Musio D, De Felice F, Raffetto N, Tombolini V, Laghi A (2015) Texture analysis as imaging biomarker of tumoral response to neoadjuvant chemoradiotherapy in rectal cancer patients studied with 3-T magnetic resonance. *Invest Radiol* 50(4):239–245. <https://doi.org/10.1097/RLL.0000000000000116>
15. De Cecco CN, Ciolina M, Caruso D, Rengo M, Ganeshan B, Meinel FG, Musio D, De Felice F, Tombolini V, Laghi A (2016) Performance of diffusion-weighted imaging, perfusion imaging, and texture analysis in predicting tumoral response to neoadjuvant chemoradiotherapy in rectal cancer patients studied with 3T MR: initial experience. *Abdom Radiol (NY)* 41(9):1728–1735. <https://doi.org/10.1007/s00261-016-0733-8>
16. Castellano G, Bonilha L, Li LM, Cendes F (2004) Texture analysis of medical images. *Clin Radiol* 59(12):1061–1069. <https://doi.org/10.1016/j.crad.2004.07.008>
17. Ahmed A, Gibbs P, Pickles M, Turnbull L (2013) Texture analysis in assessment and prediction of chemotherapy response in breast cancer. *J Magn Reson Imaging JMIR* 38(1):89–101. <https://doi.org/10.1002/jmri.23971>
18. Haralick RM, Shanmugam K, Dinstein I (2007) Textural features for image classification. In: *IEEE Xplore Document*. IEEE. <http://ieeexplore.ieee.org/document/4309314/>
19. Gourtsoyianni S, Doumou G, Prezzi D, Taylor B, Stirling JJ, Taylor NJ, Siddique M, Cook GJR, Glynne-Jones R, Goh V (2017)

- Primary rectal cancer: repeatability of global and local-regional MR imaging texture features. *Radiology*. <https://doi.org/10.1148/radiol.2017161375>
20. Jalil O, Afaq A, Ganeshan B, Patel UB, Boone D, Endozo R, Groves A, Sizer B, Arulampalam T (2017) Magnetic resonance based texture parameters as potential imaging biomarkers for predicting long-term survival in locally advanced rectal cancer treated by chemoradiotherapy. *Colorectal Dis* 19(4):349–362. <https://doi.org/10.1111/codi.13496>
 21. Nketiah G, Elschot M, Kim E, Teruel JR, Scheenen TW, Bathen TF, Selnaes KM (2017) T2-weighted MRI-derived textural features reflect prostate cancer aggressiveness: preliminary results. *Eur Radiol* 27(7):3050–3059. <https://doi.org/10.1007/s00330-016-4663-1>
 22. Kaur H, Choi H, You YN, Rauch GM, Jensen CT, Hou P, Chang GJ, Skibber JM, Ernst RD (2012) MR imaging for pre-operative evaluation of primary rectal cancer: practical considerations. *Radiographics* 32(2):389–409. <https://doi.org/10.1148/rg.322115122>
 23. Freeborough PA, Fox NC (1998) MR image texture analysis applied to the diagnosis and tracking of Alzheimer's disease. *IEEE Trans Med Imaging* 17(3):475–479. <https://doi.org/10.1109/42.712137>
 24. Yoo TS, Ackerman MJ, Lorensen WE, Schroeder W, Chalana V, Aylward S, Metaxas D, Whitaker R (2002) Engineering and algorithm design for an image processing Api: a technical report on ITK—the insight toolkit. *Stud Health Technol Inform* 85:586–592
 25. Yushkevich PA, Piven J, Hazlett HC, Smith RG, Ho S, Gee JC, Gerig G (2006) User-guided 3D active contour segmentation of anatomical structures: significantly improved efficiency and reliability. *Neuroimage* 31(3):1116–1128. <https://doi.org/10.1016/j.neuroimage.2006.01.015>
 26. Soomro MH, Giunta G, Laghi A, Caruso D, Ciolina M, Marchis CD, Conforto S, Schmid M (2017) Haralick's texture analysis applied to colorectal T2-weighted MRI: a preliminary study of significance for cancer evolution. In: *Biomedical Engineering*, 03 Feb 2017. ACTA Press, Alberta <https://doi.org/10.2316/P.2016.852-019>
 27. Wibmer A, Hricak H, Gondo T, Matsumoto K, Veeraraghavan H, Fehr D, Zheng J, Goldman D, Moskowitz C, Fine SW, Reuter VE, Eastham J, Sala E, Vargas HA (2015) Haralick texture analysis of prostate MRI: utility for differentiating non-cancerous prostate from prostate cancer and differentiating prostate cancers with different Gleason scores. *Eur Radiol* 25(10):2840–2850. <https://doi.org/10.1007/s00330-015-3701-8>
 28. Li M, Fu S, Zhu Y, Liu Z, Chen S, Lu L, Liang C (2016) Computed tomography texture analysis to facilitate therapeutic decision making in hepatocellular carcinoma. *Oncotarget* 7(11):13248–13259. <https://doi.org/10.18632/oncotarget.7467>
 29. Parmar C, Leijenaar RT, Grossmann P, Rios Velazquez E, Bussink J, Rietveld D, Rietbergen MM, Haibe-Kains B, Lambin P, Aerts HJ (2015) Radiomic feature clusters and prognostic signatures specific for lung and head and neck cancer. *Sci Rep* 5:11044. <https://doi.org/10.1038/srep11044>
 30. Inoronato M, Aiello M, Infante T, Cavaliere C, Grimaldi AM, Mirabelli P, Monti S, Salvatore M (2017) Radiogenomic analysis of oncological data: a technical survey. *Int J Mol Sci*. <https://doi.org/10.3390/ijms18040805>
 31. Ng F, Ganeshan B, Kozarski R, Miles KA, Goh V (2013) Assessment of primary colorectal cancer heterogeneity by using whole-tumor texture analysis: contrast-enhanced CT texture as a biomarker of 5-year survival. *Radiology* 266(1):177–184. <https://doi.org/10.1148/radiol.12120254>